Direct Dynamics Quasiclassical Trajectory Study of the Thermal Stereomutations of Cyclopropane

Charles Doubleday, Jr.*,†

Department of Chemistry, Columbia University, New York, New York 10027

Kim Bolton‡ and William L. Hase*,§

Department of Chemisty, Wayne State University, Detroit, Michigan 48202

Received: October 8, 1997; In Final Form: January 28, 1998

Classical trajectories are computed for the stereomutations of cyclopropane-*1,2-d*$_2$ at 695 K using direct dynamics on an AM1-SRP potential energy surface (AM1 with specific reaction parameters). The trajectories were initiated on a dividing surface, separating the cyclopropane reactants from the stereomutation products, with momenta and coordinates sampled from a 695 K Boltzmann distribution. The quasiclassical procedure was used, with two different sampling schemes, to ensure zero-point energy and vibrational quantization conditions for the energy levels on the dividing surface. From the product distribution, the ratio of rate constants for double and single methylene rotation, k_{12}/k_1, is 2.3 and 3.5 for the two sampling methods. These are between the values of 1.0 and 5−42 deduced from two separate experimental studies. A harmonic-oscillator/rigid-rotor transition-state theory calculation of k_{12}/k_1, assuming trimethylene as an intermediate, gives $k_{12}/k_1 = 1.35$ on the AM1-SRP potential energy surface. The lifetime distribution of reactive trajectories is nonexponential, in contrast to the nearly exponential decay computed from a Boltzmann average of RRKM rates. However, the initial 70% of the decay is single exponential, and the ratio of the time constants for decay of the single and double rotation rates is essentially the same as k_{12}/k_1 computed from the product ratios. Nearly all the trajectories cyclize on the first approach to a (90, 90) conformation. The data support a range of mechanistic descriptions. Most double rotations are conrotatory and occur via direct, short-lived trajectories. A quantity of 23% of trajectories have lifetimes >400 fs and include multiple independent rotations and both single and double rotation isomerizations.

I. Introduction

First reported in 1958,[1] the stereomutations of isotopically substituted cyclopropanes are an archetypal organic isomerization. An abiding question in cyclopropane isomerizations[2] is whether a trimethylene intermediate is involved and, if so, what its properties must be in order to account for the observed product distribution. In fact, there is growing evidence that small biradicals lie beyond the boundaries of what one usually means by an intermediate. An intermediate is normally assumed to exist in a local minimum on the potential energy surface (PES). However, in recent ab initio calculations with inclusion of zero-point energy (zpe), neither trimethylene[3,4,5a] nor tetramethylene[5b,6,7] lies in a minimum but they nevertheless have measurable lifetimes.[8] An intermediate with statistical dynamics should have the same properties no matter how it is generated. However, Carpenter's studies[9] of reactions where biradicals are likely to be involved point to an interpretation involving strong memory effects. A biradical with memory will have properties that depend on its precursor. A long-standing example is thermally generated tetramethylene, which shows an order of magnitude more stereorandomness when generated from cyclobutane[10] than from a diazene precursor.[11] Recently, one of us[6c] has suggested a resolution of this paradox based on dynamically determined stereochemistry.

Hoffmann's extended Hückel study[12] of trimethylene called attention to the question of single rotation vs simultaneous double rotation of the terminal methylenes. The calculation predicted that (0, 0) trimethylene (Chart 1) is an intermediate lying 10 kcal/mol below (0, 90), the presumed transition state for single rotation. Stereomutation was predicted to go via double rotation, not single rotation. Double rotation was predicted to be conrotatory because disrotation is Woodward−Hoffmann forbidden. The middle CH_2 plays the same role as the carbon lone pair in the ring opening of a cyclopropyl anion. Benson[13] concurred that trimethylene is an intermediate on the basis of bond additivity calculations and predicted trimethylene to lie in a 9.3 kcal/mol well. Early ab initio calculations of Salem[14] and Goddard[15] found a fairly flat PES with double rotation only slightly favored over single rotation. Though recent ab initio calculations on trimethylene[3,4,5a] predict the absence of a local biradical minimum when zpe is taken into account, the qualitative features of Hoffmann's PES remain: (0, 0) is lower than (0, 90) by about 1.5 kcal/mol and conrotation is favored over disrotation by about 1 kcal/mol.

One of the important goals of experiments on cyclopropane stereomutations has been to establish the ratio of double to single methylene rotation. This is important both because it serves as a test of theory and because its value could either rule out or support the involvement of a stereochemically random trimethylene intermediate. The current situation is that two careful studies of isotopically substituted cyclopropanes have yielded

† ced3@columbia.edu.
‡ kim@traj.chem.wayne.edu.
§ hase@sun.chem.wayne.edu.

S1089-5639(97)03273-8 CCC: $15.00
Published on Web 05/02/1998

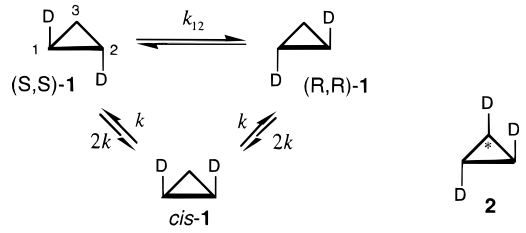

$$k = k_1 + k_1' + k_{13}$$

Figure 1. Kinetic scheme for isomerization of cyclopropane-*1,2-d*$_2$. Mechanistic rate constants are defined in the text. In **2**, * is ^{13}C.

CHART 1

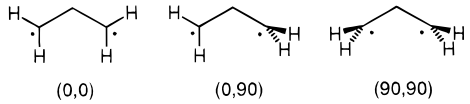

different conclusions about the mechanism of stereomutation. The point of divergence is the ratio of rate constants for approach to cis−trans equilibrium, k_i, and loss of optical activity, k_α. Berson[16] measured $k_i/k_\alpha = 1.07 \pm 0.04$ for isomerization of (*S*,*S*)-**1** at 695 K (Figure 1). The collaboration of Baldwin, Lewis, Nafie, and Freedman[17] resulted in $k_i/k_\alpha = 1.48 \pm 0.04$ from thermolysis of **2** at 680 K.[18] This apparently small difference gives rise to very different ratios of double to single rotation.

Figure 1 shows a kinetic scheme widely used to interpret k_i/k_α and the double/ single rotation rate constant ratio.[2a,16,17] Here, k_1 and k_{12} are the rate constants for net single and double CHD rotation, respectively, when the C_1-C_2 bond is cleaved. For reactions involving C_1-C_3 cleavage, k_1' is the rate constant for net single CHD rotation and k_{13} is the rate constant for double rotation of the CHD and CH_2.[19] Figure 1 leads to the following mechanistic definitions of k_i and k_α: [16]

$$k_i = 4k, \qquad k_\alpha = 2k + 2k_{12} \tag{1}$$

In the Berson experiment, the deduced value of the double/ single rotation rate constant ratio k_{12}/k_1 depends strongly on the isotope effects assumed for reaction involving C_1-C_2 vs C_1-C_3 cleavage. The isotope effects f_1 and f_{12} for single and double rotation, respectively, are given by

$$f_1 = k_1'/k_1, \qquad f_{12} = k_{13}/k_{12} \tag{2}$$

Equations 1 and 2 lead to[2a,d−f,4b,5a]

$$\frac{k_i}{k_\alpha} = \frac{2}{1 + k_{12}/k} = \frac{2 + \left(\frac{2f_{12}}{1 + f_1}\right)\frac{k_{12}}{k_1}}{1 + \left(\frac{1 + f_{12}}{1 + f_1}\right)\frac{k_{12}}{k_1}} \tag{3}$$

$$\frac{k_{12}}{k_1} = \frac{2 - \frac{k_i}{k_\alpha}}{\frac{k_i}{k_\alpha}\left(\frac{1 + f_{12}}{1 + f_1}\right) - \left(\frac{2f_{12}}{1 + f_1}\right)} \tag{4}$$

In eq 4, the ratio of mechanistic rate constants k_{12}/k_1 refers to C_1-C_2 cleavage only, deduced from the experimental ratio k_i/k_α and the assumed isotope effects.

Berson suggested $f_1 = f_{12} = 1.1$ on the basis of available precedent.[16] Getty, Davidson, and Borden[5a] and Baldwin, Yamaguchi, and Schaefer[4b] computed $f_{12} = 1.13$ and 1.12, respectively, using transition-state theory (TST) with ab initio harmonic frequencies and assuming trimethylene as an intermediate. As these authors pointed out, the computed isotope effect depends on the accuracy of the PES, and explicit consideration of the torsional potentials[3,6] may also have an effect. Putting $k_i/k_\alpha = 1.07$ and $f_1 = f_{12} = 1.1$ in eq 4 leads to $k_{12}/k_1 = 42$, but other reasonable choices could make this value much lower. If f_1 and f_{12} are uncertain within the range 0.8−1.1, the Berson experiment would be compatible with $k_{12}/k_1 = 5-42$. Even lower values of k_{12}/k_1 would be possible if one considers the upper limit of k_i/k_α compatible with the standard deviation of 0.04.[16c] In the Baldwin experiment on **2**, there is no analogous isotope effect other than the ^{13}C effect, i.e., $f_1 = f_{12} = 1$. From $k_i/k_\alpha = 1.48$,[17a] Baldwin obtained $k_{12}/k_1 = 1.0 \pm 0.2$.

The two experiments lead to very different pictures of the stereodynamics. Berson's $k_{12}/k_1 = 5-42$ suggests a moderate to negligible stereorandom component and is consistent with predominant concerted double rotation. Baldwin's $k_{12}/k_1 = 1$ is consistent with a stereorandom intermediate or with competitive concerted single and double rotations.

The kinetics of trimethylene[3] and tetramethylene[4] have been examined by microcanonical variational RRKM theory[20] and canonical variational TST[21] calculations based on ab initio PESs. Canonical variational TST calculations predict that an entropic free energy minimum of trimethylene begins to appear only at temperatures *above* 1500 K.[3b] Variational RRKM calculations predict that the trimethylene lifetime is approximately 50 fs at energies accessible at 695 K.[3a] Thus, both RRKM and TST suggest the absence of a mechanistically significant intermediate at the experimental temperature of 695 K because it lacks a free energy minimum and has a fleeting lifetime.

The power of TST is that it bypasses the dynamical details, but this is a limitation to understanding the stereochemistry of trimethylene. Dynamical aspects of the stereochemistry can be addressed with classical trajectory calculations. Chapuisat and Jean performed trajectory calculations on a PES with three degrees of freedom, and found results consistent with TST.[22] In previous work we used semiempirical direct dynamics, in which trajectories are integrated using energies and derivatives obtained directly from electronic structure theory without first fitting to an analytical function.[23] We found that trimethylene exhibits intrinsic non-RRKM decay at low energies[24a] and that the product stereochemistry depends strongly on the identity of the modes initially excited.[24b] The predicted lifetime at high energy agrees well with Zewail's experimental value.[8]

In direct dynamics calculations, use of an ab initio PES would be preferable to a semiempirical PES but is only practical for very short-time trajectory ensembles of small systems[25,26] or for single trajectories over longer times (dynamic reaction path).[27] The semiempirical direct dynamics trajectories reported here were calculated by interfacing the general dynamics program VENUS 96[28] with the MOPAC 7 semiempirical electronic structure package[29] to give the hybrid program VENUS-MOPAC.[30] The trajectories were run on a previously described[24a] AM1-SRP PES (AM1[31] with specific reaction parameters[32]).

In view of the experimental situation concerning the stereomutation dynamics, an important part of the present work is the calculation of k_i/k_α and k_{12}/k_1. An equally important goal is to find out whether trimethylene intervenes as a mechanistically significant intermediate and, if so, what its stereochemical properties are. A preliminary report of our present work on the thermolysis of cyclopropanes has appeared,[33] along with a

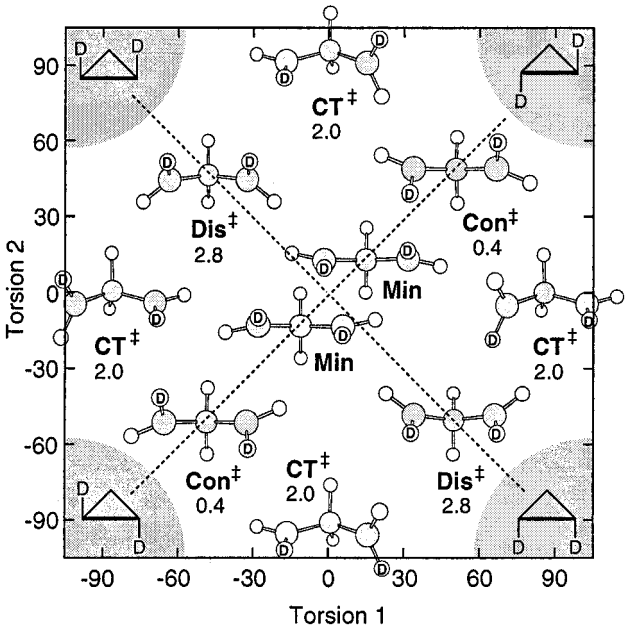

Figure 2. AM1-SRP potential energy surface for trimethylene as a function of torsion angles. Structures of stationary points are placed on the graph such that the central carbon coincides with the position of the stationary point. Conrotatory and disrotatory double rotation follow the diagonal dotted lines. Numbers beneath the names are energies in kcal/mol relative to the minima, excluding zpe. Shaded areas surrounding cyclopropanes indicate deep minima.

similar trajectory study by Hrovat, Fang, Borden, and Carpenter[34] based on an analytic fit to an ab initio PES. These two studies gave similar values for k_i/k_α and for k_{12}/k_1. We shall discuss this in detail below, but we note here that these results suggest a degree of insensitivity of the computed quantities to fine details of the trimethylene PES.

II. AM1-SRP Potential Energy Surface

This PES has been described in detail.[24a] The BIRADICAL keyword in MOPAC was used to invoke the half-electron method[35] followed by 3×3 CI involving HOMO and LUMO, and the AM1 resonance integrals between certain pairs of atoms were changed so that features of the AM1-SRP PES matched the ab initio PES. In particular, the barrier for propene formation was lowered by increasing the C−H resonance integrals involving the central hydrogens and terminal carbons, and the energies and geometries of cyclization saddle points were adjusted by scaling the resonance integrals involving both terminal carbons. The energy difference between trimethylene and the products was corrected by introducing Morse-type energy terms in the product regions of the PES.

Figure 2 summarizes the main features of the AM1-SRP PES relevant to the stereomutations of cyclopropane. From a dynamical perspective, probably the most important feature of Figure 2 is that it divides into shaded and unshaded regions. The shaded regions surround the deep cyclopropane minima. The unshaded region corresponds to trimethylene, which is free to roam throughout this region hindered only by small barriers. In particular, all the saddle points can be interconverted with only a small extra expenditure of energy. The dips and humps undoubtedly influence the motion, but the basic character of the PES is that there are deep minima separated by a high flat plateau.

Propene formation is an integral part of the AM1-SRP PES but is not included in Figure 2. Conrotatory and disrotatory double rotation follow the diagonal dotted lines. Two shallow enantiomeric minima Min (C_2 symmetry) occur along the conrotatory path, separated by a 0.01 kcal/mol barrier at the (0, 0) C_{2v} structure in the center of the diagram. Three saddle points, Con‡, Dis‡, and CT‡, mediate conrotation, disrotation, and cis−trans isomerization, respectively. On the ab initio PES,[3a,4,5a] the intrinsic reaction coordinates (IRC)[36] passing through the Con‡ and Dis‡ saddle points connect cyclopropane to shallow trimethylene minima with C_2 and C_s symmetry, respectively. The IRC passing through the ab initio CT‡ saddle point (close to (0, 90) but with C_1 symmetry) connects a pair of cyclopropanes via a single twist of the in-plane methylene and bypasses the trimethylene minima. On the AM1-SRP PES, Figure 2, Con‡ and CT‡ are saddle points and Dis‡ has two imaginary frequencies corresponding to disrotation and conrotation. The IRC passing through the AM1-SRP CT‡ saddle point ((0, 90), C_s symmetry) consists of single rotation of the out-of-plane methylene and connects two trimethylene Min structures and does not lead to cyclopropane.[24a] The CT‡−Con‡ energy difference matches the ab initio difference within 0.2 kcal/mol; the Con‡−Min energy difference equals the ab initio value. The Dis‡−Min energy difference is 2.4 kcal/mol with zpe correction, which is about 1 kcal/mol higher than its ab initio counterpart. With zpe correction, Con‡ and CT‡ are 0.4 and 1.8 kcal/mol above the two minima, Min, which merge into *one effective minimum* centered about the C_{2v} (0, 0) structure in the center of Figure 2.

The AM1-SRP relative energies are within a few tenths of a kcal/mol of the ab initio results except for the results of Dis‡. In a test of the AM1-SRP PES,[24a] direct dynamics gave a trimethylene lifetime of 90 fs, close to the experimental value of 122 ± 8 fs,[37] and variational RRKM based on AM1-SRP[24a] gave results very similar to results from variational RRKM on the ab initio PES.[3a]

III. Procedures for the Trajectory Simulations

In this study we simulate the trimethylene stereodynamics involved in thermolysis of (*S*,*S*)-**1** at high pressure, where there is a Boltzmann distribution of reacting molecules. Our goal is to determine the kinetic product distribution (relative rate constants), not the absolute rate constants. We decided not to include **2** in this study after a preliminary calculation[24b] suggested that k_{12}/k_1 is the same for **1** and **2**. Hrovat, Fang, Borden, and Carpenter[34] came to the same conclusion on the basis of an extensive comparison of their analytic PES. Unfortunately, it is not feasible to simulate the actual experiment, in which one starts and ends with cyclopropane, for two reasons. First, at 695 K the cleavage of a C−C bond is such an infrequent event that nearly all the integration time would be spent exploring cyclopropane. Second, if the dynamics of cyclopropane is ergodic, as assumed by RRKM theory, most of the trajectories in a Boltzmann distribution of cyclopropane molecules would reach the transition states for ring opening without zpe in the vibrational modes orthogonal to the reaction coordinate,[38] an unrealistic situation.

A tractable approach to simulating the high-pressure thermolysis of cyclopropane, and the one used here, is to initiate the trajectories at geometries between the cyclopropane reactant and the stereomutation products—that is, to focus on the dynamics of trimethylene rather than on cyclopropane. Intramolecular vibrational energy redistribution (IVR) is assumed to be fast for cyclopropane so that a microcanonical ensemble of reacting molecules is maintained at each energy.[39] As a result, there is a canonical Boltzmann distribution of reacting

molecules in the high-pressure thermolysis experiments. The classical rate constant for thermolysis is then a Boltzmann average of the flux of reactive trajectories through a surface that divides the cyclopropane reactant from the stereomutation products. The rate constant k is given by

$$k = \frac{1}{h^n Q_r} \int ... \int d\mathbf{q}\, d\mathbf{p}\, e^{-H(\mathbf{q},\mathbf{p})/(k_B T)} \frac{p_1}{m} \delta(q_1 - a) \chi_r(\mathbf{q}, \mathbf{p}) \quad (5)$$

where Q_r is the reactant partition function, $H(\mathbf{q}, \mathbf{p})$ is the Hamiltonian for the system as a function of coordinates $\mathbf{q}$ and momenta $\mathbf{p}$ for the n degrees of freedom ($n = 24$, excluding center-of-mass translation), q_1 and p_1 are coordinate and momentum for the degree of freedom orthogonal to the dividing surface (reaction coordinate), the Dirac delta function $\delta(q_1 - a)$ defines the dividing surface at $q_1 = a$, and $\chi(\mathbf{q}, \mathbf{p})$ is the characteristic function that equals unity if a trajectory initiated on the dividing surface moves in the reactant → product direction ($p_1 > 0$) and is reactive, and is zero otherwise. If $\chi(\mathbf{q}, \mathbf{p}) = 1$ for all trajectories initialized on the dividing surface with $p_1 > 0$, k in eq 5 becomes a TST rate constant.[21,40,41] Conventional TST is obtained if $q_1 = a$ corresponds to a first-order saddle point on the PES.

Below we discuss two different approaches used in the present calculations to model the Hamiltonian for a dividing surface separating the cyclopropane reactant from its stereomutation products. The product ratios were determined by initializing trajectories on the dividing surfaces, sampled from a Boltzmann distribution, and integrating each trajectory forward and backward until cyclopropane was formed in each direction. The relative rate of forming a given product is proportional to the number of trajectories that form the product. This is discussed in detail below.

The quasiclassical model[42] was used to sample quantum mechanical Boltzmann distributions on each dividing surface. In this method, each vibrational normal mode receives at least the zero-point energy, and any additional energy is added in discrete quanta so that the initial energy distribution for each vibrational mode is in accord with quantum mechanics. After the trajectory begins, this condition is relaxed and the system evolves according to classical mechanics. By initialization of the trajectories in this way,[42,43] the goal is to simulate the quantum mechanical relative rates for stereomutation. Previous quasiclassical trajectory simulations of IVR,[44] unimolecular decomposition from a shallow minimum,[45] and release of potential energy in going from a potential barrier to products[46] have shown that the quasiclassical trajectory model gives very good agreement with experimental results for short-time dynamical processes on the time scale of trimethylene cyclization.

A. Selection of Initial Conditions. Two different quasiclassical sampling methods, transition-state (TS) normal-mode sampling and normal-mode/rotor sampling, were used to sample Boltzmann distributions on a dividing surface separating cyclopropane from its stereomutation products.

TS Normal-Mode Sampling. In this sampling method both the vibrations and torsions are treated as normal modes, and the dividing surface intersects the saddle points on the PES connecting reactant and product cyclopropanes. Rigorously construed, this criterion is fulfilled only for Con‡ because Dis‡ is a second-order saddle point and the IRC through CT‡ connects trimethylene minima instead of cis and trans cyclopropanes (i.e., the reaction coordinate consists of single rotation of the out-of-plane methylene, but on the ab initio PES it is the in-plane methylene). However, on the AM1-SRP PES a path leading from CT‡ to cyclopropane, via rotation of the in-plane methylene, rises by no more than 0.1 kcal/mol before decreasing toward cyclopropane. Cis−trans isomerization of cyclopropane can therefore occur efficiently via CT‡ with a very small extra amount of energy. Indeed, the PES in Figure 2 is flat enough to allow Con‡, Dis‡, and CT‡ to be easily interconverted over low torsional barriers. Thus, for the 695 K sampling performed here, it is appropriate to include Con‡, Dis‡ and CT‡ as dividing surfaces.

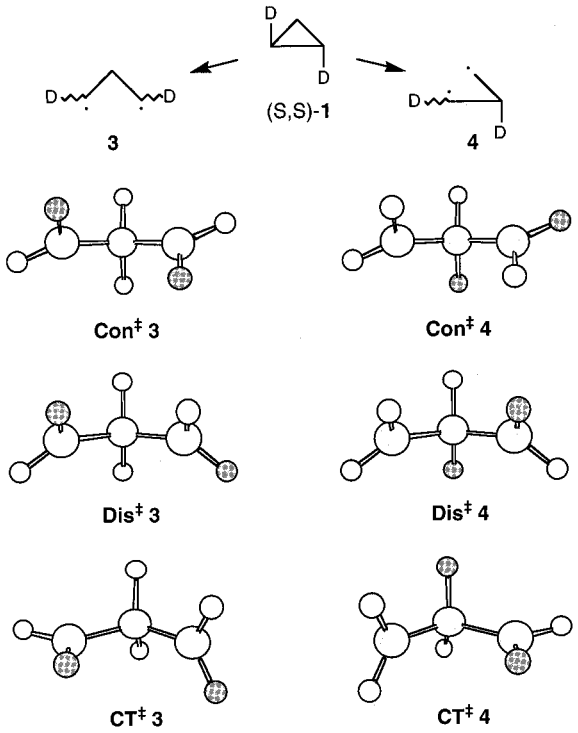

Figure 3. Starting geometries for initialization with TS normal-mode sampling. Shaded hydrogens are deuterium. Structures **3** and **4** are formed from CHD−CHD and CH_2−CHD cleavage, respectively. Con‡ and CT‡ are saddle points shown in Figure 2. Dis‡ **3** and Dis‡ **4** are nonstationary structures on the IRC just below Dis‡ (see text).

Initial conditions were chosen by an appropriate random sampling of coordinates and momenta at a specific TS structure. Sampling was initiated at the six TS structures in Figure 3, three each for CHD−CHD bond cleavage (**3**) and CHD−CH_2 cleavage (**4**). With a Boltzmann distribution of states at each TS, the relative probabilities $P_i(T)$ of populating the TSs are

$$P_{Con}(T):P_{Dis}(T):P_{CT}(T) = \frac{\lambda_{Con}}{\sigma_{Con}} Q^{\ddagger}_{Con}\, e^{-E_{Con}/(k_B T)}: \frac{\lambda_{Dis}}{\sigma_{Dis}} Q^{\ddagger}_{Dis}\, e^{-E_{Dis}/(k_B T)}: \frac{\lambda_{CT}}{\sigma_{CT}} Q^{\ddagger}_{CT}\, e^{-E_{CT}/(k_B T)} \quad (6)$$

where $Q_i^{\ddagger}$ is the partition function for TS i (CT‡, Con‡, or Dis‡), E_i is the energy difference between the zero-point levels of TS i and (*S*,*S*)-**1**, σ_i is the symmetry number for TS i, and λ_i is the number of degenerate or quasidegenerate stereoisomeric structures of TS i obtainable from (*S*,*S*)-**1** (degeneracy refers to enantiomers, and quasidegeneracy refers to diastereomers).[47] Differences among the $Q_i^{\ddagger}$ are negligible;[48] therefore, with the energy of Con‡ as the zero of energy, eq 6 becomes

$$P_{Con}(T):P_{Dis}(T):P_{CT}(T) = \frac{\lambda_{Con}}{\sigma_{Con}}: \frac{\lambda_{Dis}}{\sigma_{Dis}} e^{-(E_{Dis}-E_{Con})/(k_B T)}: \frac{\lambda_{CT}}{\sigma_{CT}} e^{-(E_{CT}-E_{Con})/(k_B T)} \quad (7)$$

Instead of initializing the trajectories by sampling all the TSs simultaneously, we calculated individual sets of trajectories for the six TSs of Figure 3. This provided more microscopic detail about the stereomutation dynamics. The results of the three sets of trajectories initiated on **3** were averaged with weights given by eq 7 to obtain the final result for isomerization of (*S*,*S*)-**1** via CHD−CHD cleavage. Similarly, the three sets of trajectories initiated on **4** were combined to give the result for CHD−CH_2 cleavage.

Because Dis‡ has two imaginary frequencies, trajectories were initialized not at Dis‡ but at a structure that had all positive eigenvalues of the projected force constant matrix,[49] located 0.7 kcal/mol below Dis‡ along the IRC for disrotatory cyclization. In this structure, CCC = 105.9° and the torsions are +55.0° and −55.0° (Dis‡ has CCC = 109.6° with torsions ±45.1°). With zpe correction this point is 2.2 kcal/mol above Min and 1.8 kcal/mol above Con‡ in Figure 2. The zpe-corrected CT‡−Con‡ energy difference is 1.4 kcal/mol.[24a]

To prepare a canonical ensemble with the zero of energy at one of the TS structures in Figure 3, the initial number of quanta n_i in each orthogonal normal mode i was selected from the harmonic quantum Boltzmann distribution function $\exp[-n_i h\nu_i/(k_B T)][1 - \exp[-h\nu_i/(k_B T)]$, where ν_i is the frequency and T = 695 K.[50] The resulting energies in the normal modes $E_i = (n_i + {}^1/_2)h\nu_i$ were transformed to normal-mode coordinates Q_i and momenta P_i by using the relations $Q_i = A_i \cos(2\pi R_i)$ and $P_i = -\omega_i A_i \sin(2\pi R_i)$ to select random phases, where $\omega_i = 2\pi\nu_i$, $A_i = (2E_i)^{1/2}/\omega_i$ is the maximum amplitude at energy E_i, and R_i is a uniform random number, $0 \le R_i \le 1$.[51,52] The initial reaction coordinate kinetic energy and momentum P_{rc} were chosen from a thermal distribution using $P_{rc} = \pm[-2k_B T \ln(1 - R)]^{1/2}$, where R is a uniform random number on [0, 1].[53] The initial Cartesian coordinates **q** and momenta **p** were obtained by transforming the Q_i and P_i and P_{rc} by the eigenvectors of the Cartesian force constant matrix. Since the normal-mode approximation is not exact for finite displacements, the selected **q** and **p** had to be scaled to obtain the desired energy for the trajectory. The scaling factor was $(E_{traj}/E_{scale})^{1/2}$, where E_{traj} is the desired energy and E_{scale} is the energy corresponding to current values of **q** and **p**. In most cases $(E_{traj}/E_{scale})^{1/2}$ is initially 1.00 ± 0.03, and the scaling was iterated 2 or 3 times until E_{scale} was within 0.1% of E_{traj}.

To create a thermal distribution of angular momentum, we assumed the TS structures were symmetric tops and sampled the angular momentum J and its z component from the probability distributions

$$P(J_z) = \exp[-J_z^2/(2I_z k_B T)] \quad 0 \le J_z \le \infty \tag{8a}$$

$$P(J) = J \exp[-J^2/(2I_x k_B T)] \quad J_z \le J \le \infty \tag{8b}$$

where I_z and I_x are the z and x components of the moment of inertia.[54] Equation 8a was sampled by rejection, and eq 8b was sampled by the cumulative distribution function[54]

$$J = [J_z^2 - 2I_x k_B T \ln(1 - R)]^{1/2} \tag{8c}$$

where R is a uniform random number on [0, 1]. J and J_z were transformed to Cartesian momenta as described previously.[51,54]

It is possible that TS normal-mode sampling introduces a bias by treating the torsions in the same way as the vibrations. In this sampling method, the Cartesian coordinates are displaced linearly along the eigenvectors of the mass-weighted Cartesian second derivative matrix. Because of the linear displacement, C−H bonds have to be stretched in order to generate a large-amplitude torsion. These spurious stretching components make the torsional barriers artificially high, which tends to suppress the amplitudes of the initial torsional displacements below what they would be without the stretching components. This problem could be solved by transforming the second derivative matrix from Cartesian to internal coordinates[55] before performing the sampling. However, an additional problem is that the vibrational amplitudes and scaling factors described above are computed in the harmonic approximation, which is not appropriate for the torsions. For these reasons we examined an alternative method for defining the reactant−product dividing surface from which initial conditions are sampled.

Normal-Mode/Rotor Sampling. In this sampling method the initial torsion angles are allowed to take on *random* values on [0, 2π] subject only to the Boltzmann condition. The rationale is that, on the periodic potential of Figure 2, trajectories starting at cyclopropane will emerge in all directions into the nearly flat trimethylene region. To minimize the bias in sampling these trajectories, we simply sampled them all instead of sampling at specific saddle points. The use of randomly sampled torsions constitutes a de facto sampling of the dividing surfaces for ring opening of (*S*,*S*)-**1**, (*R*,*R*)-**1**, and *cis*-**1**. By contrast, the Con‡ and Dis‡ structures in Figure 3 sampled by TS normal-mode sampling are on IRCs leading to (*S*,*S*)-**1**. This in itself should have no effect on the computed relative rate constants in Figure 1.

Normal-mode/rotor sampling was used to initialize two sets of trajectories, for **3** and **4**. In this method, the molecule is assumed to consist of 19 nontorsional vibrations plus two torsions. The torsions are unrestricted over [0, 2π] and sampled by a thermal Monte Carlo scheme,[56] and the nontorsional modes are sampled by the TS normal-mode sampling described above. To implement the method, it is necessary to choose a reference structure on the dividing surface at which to compute the nontorsional frequencies, which are assumed to be independent of the torsions and invariant over the dividing surface. In fact, the nontorsional modes of CT‡, Con‡, and Dis‡ are virtually invariant,[57] but to minimize any variations, we chose a lower energy structure well on the way to cyclization as the reference structure for the nontorsional modes. Therefore, the sampling was started from a geometry located 0.4 kcal/mol below Con‡ along the IRC for conrotatory cyclization toward cyclopropane. At this geometry the CCC angle is 105°, down from 109° at Con‡.[24a]

Diagonalization of the force constant matrix of the reference structure yielded $3N - 7 = 20$ eigenvalues after projecting out[49] translations, rotations, and gradient (the conrotatory reaction path). The lowest was disrotatory torsion and was excluded from the set of nontorsional modes. Initial Cartesian coordinates and momenta for the 19 nontorsional modes were chosen with TS normal-mode sampling as described above. The combined energy of the two torsions, E_{tor}, was then sampled from a mean energy of $2k_B T$ (the reaction coordinate with mean energy $k_B T$,[58] plus the classical vibrator limit[50] $k_B T$ of the other torsion) by choosing from $E_{tor} = -2k_B T \ln R$, where R is a uniform random number on [0, 1]. Starting from the geometry produced by TS normal-mode activation of the nontorsional modes, the torsions were activated by first displacing each by a random rotation on [0, 2π] followed by 2000 steps of a Markov chain using the Metropolis algorithm[56] with Boltzmann weighting. The random walk was performed in internal coordinates, varying only the two torsions.[59] At this point the combined torsional kinetic energy was given by $T_{tor} = E_{tor} - (V_{vt} - V_v)$, where V_v is the potential energy following TS normal-mode sampling of the

nontorsional vibrations, and V_{vt} is the potential energy after the 2000 step torsional random walk. Individual torsions were given kinetic energy $T_1 = RT_{tor}$ and $T_2 = T_{tor} - T_1$, where R is a freshly generated uniform random number. From the torsional angular momenta $J_i = \pm(2I_iT_i)^{1/2}$ ($i = 1, 2$), we computed angular velocities $\Omega_i = J_i/I_i$, where I_i is the reduced moment of inertia for torsion i. We used $I_{CHD} = 2.48$ and $I_{CH_2} = 1.68$ amu Å^2. The angular velocities were then used to compute $\mathbf{p}_i = \mathbf{M}_i(\Omega_i \times \mathbf{r}_i)$, the six-component torsional contribution from torsion i to the full Cartesian momentum, where $\mathbf{M}_i$ is the 6×6 diagonal matrix of atomic masses of the two H/D atoms of torsion i (three identical elements for each atom) and $\mathbf{r}_i$ is their Cartesian position vector.

A complication introduced by this method of torsional activation is that the momenta originally selected by TS normal-mode activation of the nontorsional modes are no longer appropriate for the torsionally activated molecule. For example, momentum originally placed in a C−H stretch becomes largely torsional momentum if the C−H bond is rotated by 90° during torsional activation. Therefore, before adding the $\mathbf{p}_i$ contributions described above, we rotated the nine Cartesian momentum components of each terminal CH_2 or CHD group through their respective cumulative angles produced by the torsional random walk. The main effect was to preserve the local character (C−H stretch, CCH bend, etc.) of the momenta initially placed in the terminal methylenes by TS normal-mode sampling of the nontorsional modes. After subtracting any overall rotational angular momentum artificially created during the torsional random walk, we multiplied the Cartesian momentum by the scaling factor $[(E_v + E_{tor} - V_{vt})/T_{vt}]^{1/2}$ to produce a total energy equal to $E_{tor} + E_v$, where E_v is the total energy resulting from TS normal-mode vibrational activation and T_{vt} is the kinetic energy after vibrational and torsional activation. The scaling factor was usually 1.00 ± 0.03. Finally, the molecule was rotationally activated at 695 K according to eq 8.

If TS normal-mode sampling tends to restrict the initial torsions to the vicinity of the saddle points, normal-mode/rotor sampling may tend to err in the opposite direction by allowing the initial torsion angles to take on random values. By selecting initial conditions with these two sampling schemes, we hope to bracket the true Boltzmann distribution for the cyclopropane ring opening TSs on the AM1-SRP PES.

B. Trajectory Integration. The atomic motion was evaluated by integrating Hamilton's equations in Cartesian coordinates and momenta with a combined 4th-order Runge−Kutta and 6th-order Adams−Moulton predictor−corrector algorithm,[60] as implemented in VENUS 96.[28] At each step of the integration the Schroedinger equation was solved according to the AM1-SRP prescription.[24a] The first derivative of the energy with respect to Cartesian positions was computed by the Dewar−Liotard[61] analytical CI method in MOPAC 7. The integration step size was 0.25 fs, and energy was conserved to four or five significant figures over a typical trajectory. All computations were performed on the IBM SP2 at the Cornell Theory Center.[62] The integration rate was 16.5 fs of trimethylene motion per CPU minute per node (RS6000 Power 2).

C. Final Trajectory Conditions. Each trajectory was integrated forward and backward in time until either propene or cyclopropane was formed. In this way, the product distribution was obtained by following each cyclopropane isomerization until it completed its journey through the biradical region of the PES. The criterion for propene formation was that the breaking C−H bond was at least 2.3 Å and the nascent C−H bond was shorter than 1.3 Å. For cyclization, the trajectory was stopped when the CCC angle dropped below 70°.

IV. Analysis of Trajectories

To compute the relative rates of isomerization among (*S*,*S*)-**1**, (*R*,*R*)-**1**, and *cis*-**1** and the ratio of double to single methylene rotation, the main task was to count the net rotations needed to interconvert the products formed in the forward and backward trajectory segments. For a given CHD group, only trajectories that connect cyclopropane isomers via an odd number of 180° rotations correspond to observable events. Trajectories in which both reactant and product were the same were deemed unreactive even if extensive rotations (by even multiples of 180°) had taken place. In monitoring single vs double rotation, we recorded a double rotation only if both methylenes rotated by an odd multiple of 180°. An isomerization in which one rotated by 180° and the other by 360° was counted as single rotation. For CHD−CHD cleavage via **3**, double rotation connects (*S*,*S*)-**1** with (*R*,*R*)-**1** and single rotation connects trans with cis. For CH_2−CHD cleavage via **4**, both double rotation and single CHD rotation connect trans with cis.

For the trajectories initialized with TS normal-mode sampling, the rate constant ratio of double to single rotation, k_{12}/k_1, is

$$\frac{k_{12}}{k_1} = \frac{G_{12}}{G_1} \tag{9}$$

where G_1 and G_{12} are Boltzmann weighted product yields for the single and double rotation processes labeled k_1 and k_{12} in Figure 1 averaged over the results obtained from sampling at Con‡ **3**, Dis‡ **3**, and CT‡ **3** in Figure 3. That is, G_1 is half the yield of (*S*,*S*)-**1** → *cis*-**1** (from the factor of 2 in Figure 1) and G_{12} is the yield of (*S*,*S*)-**1** → (*R*,*R*)-**1**, both via **3**. k_{12}/k, which is used in eq 3 to compute the experimental ratio k_i/k_α, is obtained from the trajectory results by

$$\frac{k_{12}}{k} = \frac{G_{12}}{G_1 + G'} \tag{10}$$

where G' is the yield for (*S*,*S*)-**1** → *cis*-**1** via both single and double rotation in **4** (processes with rate constants k_1' and k_{13} in Figure 1) Boltzmann averaged over the trajectories sampled at Con‡ **4**, Dis‡ **4**, and CT‡ **4** with relative weights according to eq 7. Thus, eq 10 combines the trajectory results for **3** and **4**, assuming zero isotope effect on the formation of **3** and **4** from cyclopropane. Boltzmann weighting factors W_{Dis} and W_{CT} are calculated relative to Con‡ using zpe-corrected energies $E_{Dis} - E_{Con} = 1.8$ and $E_{CT} - E_{Con} = 1.4$ kcal/mol,

$$W_{Con} = 1 \tag{11a}$$

$$W_{Dis} = \frac{\lambda_{Dis}/\sigma_{Dis}}{\lambda_{Con}/\sigma_{Con}} e^{-(E_{Dis}-E_{Con})/(k_BT)} \tag{11b}$$

$$W_{CT} = \frac{\lambda_{CT}/\sigma_{CT}}{\lambda_{Con}/\sigma_{Con}} e^{-(E_{CT}-E_{Con})/(k_BT)} \tag{11c}$$

where the explicit dependence of λ and σ on D substitution (**3** vs **4**) is not shown. For **3**, $\lambda_{Con} = \lambda_{CT} = 2$, $\lambda_{Dis} = 1$, $\sigma_{Con} = 2$, $\sigma_{Dis} = \sigma_{CT} = 1$, $W_{Dis} = 0.27$, $W_{CT} = 0.72$ at 695 K. For **4**, $\lambda_{Con} = \lambda_{Dis} = \lambda_{CT} = 2$, $\sigma_{Con} = \sigma_{Dis} = \sigma_{CT} = 1$, $W_{Dis} = 0.27$, $W_{CT} = 0.36$ at 695 K.

The product yields are given by

$$G_1 = \frac{P^{ct}_{Con3} + W_{Dis}P^{ct}_{Dis3} + W_{CT}P^{ct}_{CT3}}{2(1 + W_{Dis} + W_{CT})} \quad (12a)$$

$$G_{12} = \frac{P^{opt}_{Con3} + W_{Dis}P^{opt}_{Dis3} + W_{CT}P^{opt}_{CT3}}{1 + W_{Dis} + W_{CT}} \quad (12b)$$

$$G' = \frac{P^{ct}_{Con4} + W_{Dis}P^{ct}_{Dis4} + W_{CT}P^{ct}_{CT4}}{1 + W_{Dis} + W_{CT}} \quad (12c)$$

where P^i_j is the fractional yield for process i (cis−trans isomerization, ct, or optical isomerization, opt) derived from TS normal-mode sampling at TS structure j (one of the 6 structures in Figure 3), calculated assuming (*S*,*S*)-**1** as the reactant. P^i_j is defined by

$$P^i_j = \left(\frac{N_i}{N_{SS}}\right)_j \quad (13)$$

where N_i is the number of trajectories that undergo process i and N_{SS} is the number that forms (*S*,*S*)-**1** in at least one of the forward-time or backward-time trajectory segments. For example, of all the trajectories initialized at Con‡ **3**, P^{ct}_{Con3} is the fraction involving cis−trans isomerization of (*S*,*S*)-**1**, i.e., in which either the forward or backward segment leads to (*S*,*S*)-**1** and the other segment leads to *cis*-**1**. N_{SS} is analogous to a reactant concentration. The factor of 2 appears in eq 12a because in Figure 1 the rate constant for (*S*,*S*)-**1** → *cis*-**1** via **3** is $2k_1$, so the yield for this reaction must be divided by 2 to reflect k_1.

The procedure for obtaining kinetic product ratios from normal-mode/rotor sampling is similar to eqs 9 and 10. The ratio k_{12}/k in terms of the product yields is

$$\frac{k_{12}}{k} = \frac{F_{12}}{F_1 + F'} \quad (14)$$

where F_1, F_{12}, and F' are the normal-mode/rotor analogues of G_1, G_{12}, and G'. The double/single rotation rate constant ratio is

$$\frac{k_{12}}{k_1} = \frac{F_{12}}{F_1} \quad (15)$$

the analogue of eq 9. Equation 3 is used to calculate k_i/k_α using eq 14 in the case of normal-mode/rotor sampling or using eq 10 in the case of TS normal-mode sampling. Because Boltzmann weighting is part of the normal-mode/rotor sampling scheme, F_1, F_{12}, and F' are obtained directly from the trajectories by a procedure presented below.

V. Results and Discussion

A. Product Ratios. In this discussion, "trajectory" refers to the combined forward-time and backward-time segments from a given set of initial coordinates and momenta. Table 1 shows the results from the TS normal-mode sampling method. N_{tot} is the total number of trajectories, N_{pr} is the number that form propene, N_{ct} is the number that interconvert (*S*,*S*)-**1** and *cis*-**1**, $N_{opt} = N_{con} + N_{dis}$ is the number that undergo optical isomerization by conrotation (N_{con}) or disrotation (N_{dis}), and N_{SS} is the number that form (*S*,*S*)-**1** in at least one of the forward/backward trajectory segments. These are used in eqs 12 and 13 to compute the Boltzmann averaged product yields.

TABLE 1: Results from TS Normal-Mode Sampling

barrier and H/D pattern[a]	N_{tot}[b]	N_{pr}[c]	N_{SS}[d]	N_{opt}[e]	N_{ct}[f]	N_{con}[e]	N_{dis}[e]
Con‡ **3**	133	13	98	59	21	52	7
Dis‡ **3**	120	3	93	36	43	23	13
CT‡ **3**	158	12	60	17	38	4	13
Con‡ **4**	78	6	58		43		
Dis‡ **4**	80	4	64		28		
CT‡ **4**	80	6	66		48		

[a] See Figure 3. [b] Total no. of trajectories. [c] No. of trajectories that form propene. [d] No. of trajectories that form (*S*,*S*)-**1** in at least one of the forward−backward trajectory segments. [e] $N_{opt} = N_{con} + N_{dis}$ is the number that undergoes optical isomerization by conrotation or disrotation. [f] No. of trajectories that interconvert (*S*,*S*)-**1** and *cis*-**1**.

The trajectory counts from normal-mode/rotor sampling are shown in Table 2 and Figure 4. N_{SS}, N_{RR}, and N_{cis} are the number of trajectories that formed (*S*,*S*)-**1**, (*R*,*R*)-**1**, and *cis*-**1** in at least one of the forward/backward trajectory segments and are shown in parentheses beneath each structure in Figure 4. $N_{i,j}$ (i, j = RR, SS, cis) is the number of trajectories that interconvert isomers i and j. The other column headings have the same meaning as in Table 1. Equations 16−18 define F_1 and F_{12}, the mean fraction of single and double rotation via **3**, and F', the average yield for interconversion of *cis*-**1** and (*S*,*S*)-**1** via **4**,

$$F_1 = \frac{1}{4}\left(\frac{N_{SS,cis}}{N_{cis}} + \frac{N_{RR,cis}}{N_{cis}} + \frac{N_{SS,cis}}{2N_{SS}} + \frac{N_{RR,cis}}{2N_{RR}}\right) \quad (16)$$

$$F_{12} = \frac{1}{4}\left(\frac{N_{SS,RR}}{N_{SS}} + \frac{N_{SS,RR}}{N_{RR}} + \frac{N_{cis,cis}}{N_{cis1}} + \frac{N_{cis,cis}}{N_{cis2}}\right) \quad (17)$$

$$F' = \frac{1}{2}\left(\frac{N_{ct}}{N_{cis}} + \frac{N_{ct}}{N_{SS}}\right) \quad (18)$$

where N_{cis1} and N_{cis2} are the numbers of trajectories that form the two species of *cis*-**1** shown at the left in Figure 4 ($N_{cis1} + N_{cis2} = N_{cis}$). The data are averaged because of the small number of trajectories. Each equation is the mean of the different ways (four, four, and two ways, respectively) of using the data to calculate the quantity on the left. In the limit of perfect statistics the cis−trans cyclopropane equilibrium constant is unity and $N_{SS} = N_{RR} = N_{cis}/2$, $N_{SS,cis} = N_{RR,cis}$, $N_{SS,RR} = N_{cis,cis}$. Then substitution of eqs 16 and 17 into eq 15 would give $F_{12}/F_1 = 2N_{SS,RR}/N_{SS,cis}$. In eq 17 the experimentally unobservable cis−cis reaction is included to improve the statistics for double rotation. The factors of 2 appear in eq 16 for the same reason as in eq 12a.

Table 3 shows the product yields and rate constant ratios computed from both sampling methods. The reactive fractions are less with normal-mode/rotor sampling than with TS normal-mode sampling ($F_1 < G_1$, $F_{12} < G_{12}$, $F' < G'$) in part because normal-mode/rotor sampling was initiated 0.4 kcal/mol below Con‡. The computed value of k_i/k_α (1.32 and 1.28) is midway between the value of 1.07 ± 0.04 reported by Berson[16] for isomerization of **1** and 1.48 ± 0.04 reported by Baldwin[17a] for isomerization of **2**. Our value of k_{12}/k_1, 2.3−3.5, is also midway between the 1.0 of Baldwin and the 5−42 range compatible with the Berson experiment. A computed value of k_{12}/k_1 close to both experiments suggests that direct dynamics on AM1-SRP gets the main features of the dynamics correct, but there emerges no clear support or rejection of either the Berson or

TABLE 2: Results from Normal-Mode/Rotor Sampling[a]

d_2 pattern	N_{tot}	N_{pr}	N_{SS}	N_{RR}	N_{cis}	$N_{RR,cis}$	$N_{SS,cis}$	$N_{RR,SS}$	$N_{cis,cis}$	N_{opt}	N_{ct}	N_{con}	N_{dis}
3	960	44	330	351	619	66	76	135	116	135	142	113	22
4	260	9	179		172		172				102	77	16

[a] $N_{i,j}$ (i, j = RR, SS, cis) is the number of trajectories that interconvert isomers i and j (eqs 16−18). Others have the same meaning as in Table 1.

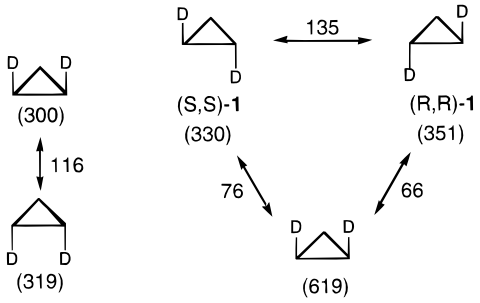

Figure 4. Number of trajectories that connect each pair of isomers initiated on **3** with normal-mode/rotor sampling. Numbers in parentheses under each isomer are the total number of trajectories that lead to that isomer, including unreactive trajectories that form the given isomer in both the forward and backward directions. The unobservable cis−cis reaction is shown at left.

Baldwin picture of the stereodynamics. Recently, Hrovat, Fang, Borden, and Carpenter[34] reported a trajectory study of cyclopropane stereomutations on an analytical PES. Like AM1-SRP, their PES is a good but not perfect approximation to the ab initio PES. The two PESs differ from ab initio in different ways,[63] but they give similar values of k_{12}/k_1. At 695 K, the $k_{12}/k_1 = 4.7$ of Hrovat et al. is close enough to our 2.3−3.5 to suggest a robust system in which the stereodynamics are not extremely sensitive to the subtleties of the PES but to broader features of the PES.

B. TST Prediction of k_{12}/k_1. Given the features of the AM1-SRP PES, statistical theory can be applied to predict k_{12}/k_1 for concerted and nonconcerted mechanisms of cyclopropane stereomutations. The TST estimates are based on eqs 6 and 7, in which the differences among Con‡, Dis‡, and CT‡ harmonic partition functions are negligible,[48] and conventional TST rather than variational TST is used. The concerted mechanism, with no trimethylene intermediate, is shown in Figure 1. With (*S*,*S*)-**1** as reactant, crossing Con‡ **3** or Dis‡ **3** gives (*R*,*R*)-**1** and crossing CT‡ **3** gives *cis*-**1**. From eq 7, the resulting k_{12}/k_1 ratio at 695 K is

$$\frac{k_{12}}{k_1} = \frac{\dfrac{\lambda_{Con}}{\sigma_{Con}} + \dfrac{\lambda_{Dis}}{\sigma_{Dis}} e^{-(E_{Dis}-E_{Con})/(k_B T)}}{\dfrac{\lambda_{CT}}{\sigma_{CT}} e^{-(E_{CT}-E_{Con})/(k_B T)}} = 1.77 \qquad (19)$$

smaller than the 2.3−3.5 ratio deduced from the trajectory results. In the limit that the energy differences in eq 19 approach zero, k_{12}/k_1 approaches 1. The difference from unity is due to the Boltzmann factors.

One can also make a TST prediction with the assumption that trimethylene intervenes as a reactive intermediate. Figure 5 shows such a scheme with relative rate constants given in terms of Boltzmann factors B_{Con}, B_{Dis}, and B_{CT}. On AM1-SRP, **3a**−**3c** cyclize via Con‡ or Dis‡ and undergo stereochemical interconversion (but not cyclization) via CT‡. From eq 7, the relative rates of formation of **3a**−**3c** from (*S*,*S*)-**1**, k_a, k_b, k_c (not included in Figure 5), are

$$\frac{k_b}{k_a} = \frac{k_b}{k_c} = \frac{\lambda_{Dis}/\sigma_{Dis}}{\lambda_{Con}/\sigma_{Con}} e^{-(E_{Dis}-E_{Con})/(k_B T)} = 0.54 \qquad (20)$$

Steady-state analysis of the kinetic scheme leads to $k_{12}/k_1 = 1.35$, below the 2.3−3.5 in Table 3. From a kinetic scheme involving a trimethylene intermediate on their analytical PES, Hrovat, Fang, Borden, and Carpenter[34] deduced a TST prediction of $k_{12}/k_1 = 1.18$, also below their trajectory-derived value of 4.7. Baldwin, Yamaguchi, and Schaefer[4b] also used a kinetic scheme with a trimethylene intermediate to compute $k_{12}/k_1 = 0.94$ directly from their ab initio PES.

Since the k_{12}/k_1 ratios in Table 3 exceed the TST estimates of 1.35 and 1.77, the trajectories appear to exhibit a dynamical preference for double over single rotation. However, the trajectory calculations are anharmonic and the TST estimates are based on harmonic partition functions for the nontorsional modes.[48] A fully anharmonic TST estimate[64] may be different. At present the contribution of nonstatistical dynamics to the product distribution is not known. However, at a fixed energy of 4.4 kcal/mol above the zero-point level, trajectories initiated at Con‡ exhibit high mode selectivity in favor of conrotation as long as the initial energy placed into disrotation is low.[24a]

C. Trimethylene Unimolecular Kinetics. Figure 6 shows the survival probability $S(t) = N(t)/N_0$ and lifetime distribution $P(t) = -(1/N_0)\, dN(t)/dt$ of the trajectories computed for **3** with normal-mode/rotor sampling, where $N(t)$ is the number of trajectories that have not formed product at time t and $N_0 = 959$ is the total number at $t = 0$. For a given trajectory the lifetime was taken to be the sum of the duration of the forward and backward trajectory segments, delimited in each direction by the final passage through the TS. This is the total time spent traversing the trimethylene region of the PES, from ring opening to product formation. Our TS criterion for cyclization was CCC = 94°, determined previously[24a] for energies in this range.[65]

The decay in Figure 6 is strongly nonexponential. For $t <$ 100 fs, about 40% of the biradicals decay with a time constant $\tau \approx 60$ fs, where τ is the reciprocal of the time constant for decay of $P(t)$ (to be distinguished from the individual trajectory lifetimes). This early decay is almost entirely due to unreactive trajectories that enter the trimethylene region and promptly cyclize to reactant. It might arise in part from our choice of reference structure for normal-mode/rotor sampling that is 0.4 kcal/mol below Con‡. In the range $100 < t < 550$ fs, $P(t)$ decays with $\tau \approx 230$ fs; this includes most of the reactive trajectories. Above 600 fs the survival probability of the remaining 15% of the trajectories (about half reactive) decays with $\tau \approx 600$ fs. The decay extends into the multipicosecond range—7% of the trajectories last 1−4 ps. The large range of decay rates indicates substantial nonstatistical character in the dynamics.

For a comparison to these lifetimes, it is useful to have an estimate of the time it takes a CHD group to rotate at 695 K. For a rotor with mean kinetic energy $k_B T$ (the mean energy of a reaction coordinate[58]) the angular velocity, $(2k_B T/I)^{1/2}$, is 2.2 $\times 10^{13}$ radian s^{-1} for a CHD with a reduced moment of inertia

TABLE 3: Product Yields and Rate Constant Ratios Defined in Eqs 9−18

sampling method	G_1	G_{12}	G'	F_1	F_{12}	F'	k_{12}/k	k_{12}/k_1	k_i/k_α
TS normal mode	0.20	0.46	0.70				0.51	2.3	1.32
normal-mode/rotor				0.11	0.39	0.58	0.56	3.5	1.28

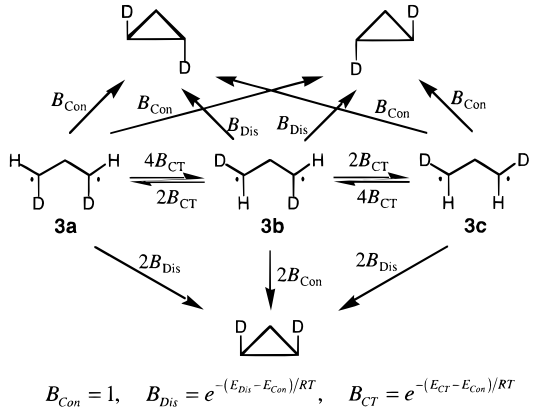

Figure 5. Reaction scheme for nonconcerted cyclopropane stereomutations used for TST prediction of k_{12}/k_1. Relative rate constants are given as multiples of the Boltzmann factors B_{Con}, B_{Dis}, and B_{CT}, multiplied by λ/σ as in eq 7. For **3a**−**3c**, $\sigma_{3a} = \sigma_{3c} = 2$, $\sigma_{3b} = 1$. A count of stereoisomeric pathways gives $\lambda_{Con} = 2$, $\lambda_{Dis} = 1$, $\lambda_{CT} = 2$ for all reactions shown. For the TSs, conrotation of **3a** or **3c** has $\sigma = 2$ and all others have $\sigma = 1$.

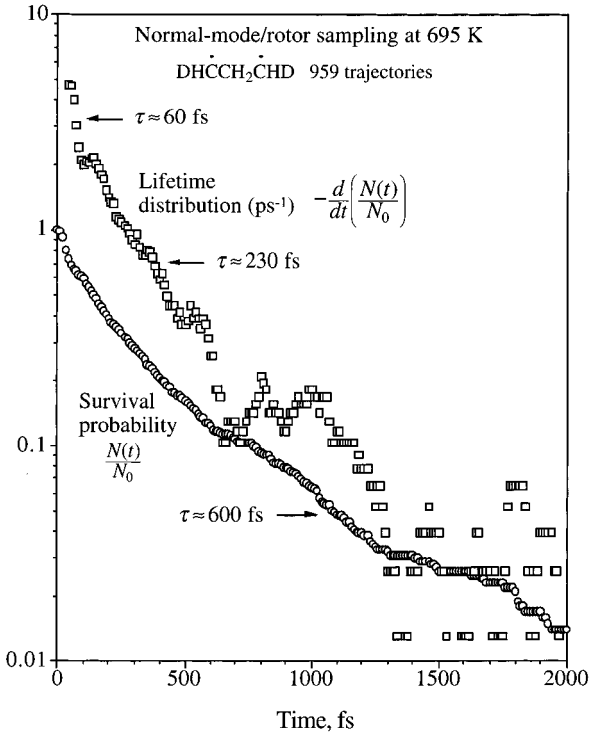

Figure 6. Lifetime distribution $P(t)$/ps^{-1} and survival probability $S(t)$ (definitions in text) for trajectories initiated with normal-mode/rotor sampling on **3**. Approximate time constants τ were fitted to a single exponential within a specific range described in the text.

I of 2.48 amu Å^2. The resulting mean time for a 180 ° CHD rotation is 140 fs, close to Zewail's 122 ± 8 fs lifetime for trimethylene-d_0 at high energy.[37]

At 695 K, the RRKM prediction for $S(t)$ is a Boltzmann average,

$$S(t) = \int_{E_{Con}}^{\infty} e^{-k(E)t} P(E)\, dE \qquad (21)$$

where $k(E)$ is the RRKM rate constant and $P(E)$ is the

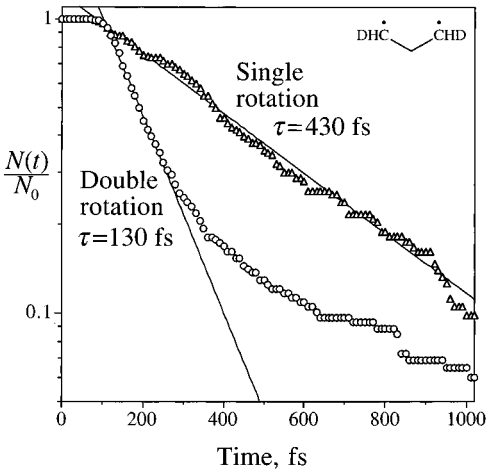

Figure 7. Survival probabilities of single and double rotation reactive trajectories initiated on **3** with normal-mode/rotor sampling. Double rotation includes both optical isomerization and cis-to-cis trajectories. Fits to a single exponential were made between 100 and 900 fs for single rotation (τ = 430 fs) and between 100 and 250 fs for double rotation (τ = 130 fs).

normalized probability that trimethylene has energy E, determined by the Boltzmann distribution sampled in choosing the initial conditions. Though eq 21 suggests nonexponential decay, $S(t)$ computed in this way is nearly exponential. This is because the very low barriers make cyclization so efficient that $k(E) \approx 1.4 \times 10^{12}$ s^{-1} over the entire range of E accessible at 695 K.

Figure 7 shows the survival probabilities $S(t)$ for the *reactive* trajectories of **3** initiated with normal-mode/rotor sampling; i.e., trajectories whose forward and backward segments led to different cyclopropane isomers. The triangles represent net single rotation (cis−trans) and the circles double rotation, including optical isomerization and the formally unobservable cis-to-cis double rotation (included to improve the statistics). The single and double rotation trajectories have very different time constants (τ) for decay. Their ratio is $^{430}/_{130} = 3.3$, essentially the same as the $k_{12}/k_1 = 3.5$ derived from product ratios. The two ratios would be identical if each decay was exponential. However, in contrast to the RRKM prediction of single-exponential decay, the decay of double rotation trajectories in Figure 7 is highly nonexponential. It may be that single rotation trajectories persist longer in the trimethylene region of the PES simply because they have to surmount a higher barrier than conrotatory double rotation. Trajectories undergoing disrotatory double rotation, which has a higher barrier than single rotation on the AM1-SRP PES, also decay with a long time constant on the order of a single rotation decay. The number is uncertain because there are only 42 trajectories.

In the vast majority of cases, a trajectory cyclizes the first time it comes close to a (90, 90) conformation. Most double rotation trajectories undergo a single set of approximately simultaneous 180° rotations and cyclize immediately. The common feature of most long-lived trajectories, whether single or double rotation, is a mismatch of torsional phases that frustrates a (90, 90) alignment and prolongs the trajectory. We base this on a survey of reactive and unreactive trajectories lasting >500 fs, 84% of which cyclize on the first approach to (90, 90) even though each torsion may undergo several 180°

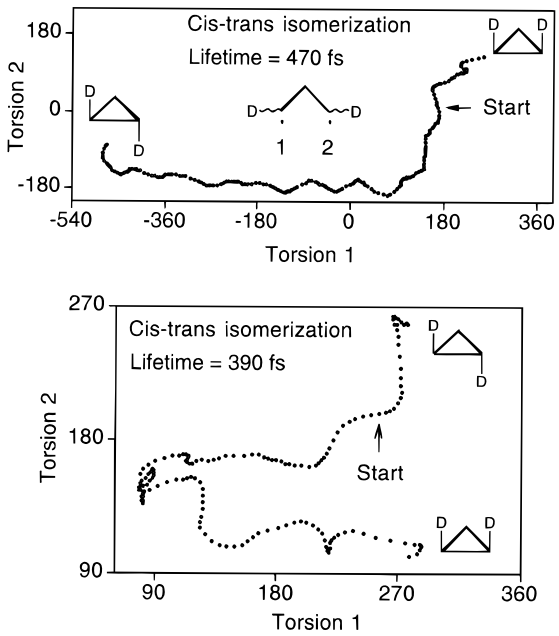

Figure 8. Torsion angles (degrees) for two cis−trans isomerization trajectories plotted every 2.5 fs.

rotations. Of the 16% that pass at least once through (90, 90) without cyclizing, half have an unfavorably large CCC angle at that point in the trajectory, and over 80% started off with an exceptionally large torsional energy (maintained throughout the long trajectory) that tends to carry them through the (90, 90) region without cyclizing.

Two typical trajectories showing net single rotation are shown in Figure 8, initiated by normal-mode/rotor sampling on **3**. In the upper plot, a single rotation of 3π and a conrotatory double rotation combine to give net single rotation. In this case and in many others the rotational displacement is nearly linear with time over a large fraction of the trajectory, a manifestation of weak coupling of the torsions to the other modes (except the strongly coupled CCC bend), consistent with the highly structured power spectrum.[24a] This description applies to most of the conrotatory trajectories, which are basically direct. In other cases, as in the lower plot, one or more sections of the trajectory appear to wander randomly. This trajectory shows a clear case of nonzero torsional−nontorsional coupling in the left part of the plot where torsion 1 reverses its direction.

D. Mechanism of Stereomutation. The distribution of lifetimes and decay constants in Figures 6 and 7 implies a mechanistic continuum encompassing concerted and nonconcerted. In classifying the mechanism, one could adopt the criterion that a species detectable by transient spectroscopy[8] must be an intermediate. However, the majority of double rotation trajectories could hardly be more direct. These trajectories have time to do little else but open the ring, rotate, and cyclize. Since the enantiomerization reaction, (*S*,*S*)-**1** → (*R*,*R*)-**1**, takes place mainly by way of these trajectories, we would describe it as primarily, though not exclusively, concerted.

A significant minority of reactive trajectories are long-lived (23% live over 400 fs) and include multiple independent rotations and both single and double rotation isomerization channels—features one expects of an intermediate. However, such an intermediate may not behave statistically because the polyexponential decay in Figures 6 and 7 is incompatible with statistical dynamics for the ensemble as a whole. An unanswered question is whether the short-lived trajectories are mainly responsible for the nonstatistical dynamics, and the long-lived trajectories behave essentially statistically. Carpenter[9a] has used this assumption to compute a bimodal lifetime distribution in a direct dynamics quasiclassical trajectory study of a [1,3]-sigmatropic shift, where the long-lived component was computed from RRKM theory. The product ratios of the trajectories in Figure 7 that last >400 fs are consistent with the possibility of statistical dynamics for long-lived trajectories. They give $k_{12}/k_1 \approx 1.4$, similar to the harmonic TST value of 1.35 for the case of a trimethylene intermediate. Further assessment of statistical behavior for the long-lived trajectories will require including anharmonic effects, particularly for the torsions (for example, as in ab initio calculations of trimethylene[3a] and tetramethylene[6c]), when determining the TST value for k_{12}/k_1.

Acknowledgment. C.D. is grateful for financial support from the National Science Foundation and for a grant of time on the IBM SP2 at the Cornell Theory Center. K.B. and W.L.H. are grateful for financial support from the National Science Foundation, CHE-94-03780. The authors greatly appreciate helpful discussions with Professors J. E. Baldwin, J. A. Berson, B. K. Carpenter, and W. T. Borden.

References and Notes

(1) Rabinovitch, B. S.; Schlag, E. W.; Wiberg, K. B. *J. Chem. Phys.* **1958**, *28*, 504.

(2) (a) Baldwin, J. E. In *The Chemistry of the Cyclopropyl Group*; Rappoport, Z., Ed.; Wiley: Chichester, 1995; Vol 2, pp 469−494. (b) Berson, J. A. *Science* **1994**, *266*, 1338. (c) Boche, G.; Walborsky, H. M. *Cyclopropane Derived Reactive Intermediates*; Wiley: Chichester, 1990. (d) Carpenter, B. K. In *The Chemistry of the Cyclopropyl Group*; Rappoport, Z., Ed.; Wiley: Chichester, 1987; Part 2, pp 1027−1082. (e) Borden, W. T. In *Reactive Intermediates*; Jones, M., Moss, R. A., Eds.; Wiley: New York, 1985; Vol. 3, pp 151−188; 1981; Vol. 2, pp 175−209. (f) Carpenter, B. K. *Determination of Reaction Mechanisms*; Wiley: New York, 1984; pp 62−67. (g) Dervan, P. D.; Dougherty, D. A. In *Diradicals*; Borden, W. T., Ed.; Wiley: New York, 1982; Chapter 3. (h) Gajewski, J. J. *Hydrocarbon Thermal Isomerizations*; Academic: New York, 1981; pp 27−42. (i) Berson, J. A. In *Rearrangements in Ground and Excited States*; deMayo, P., Ed.; Academic: New York, 1980; Vol. 1, pp 311−390.

(3) (a) Doubleday, C. *J. Phys. Chem.* **1996**, *100*, 3520−3526. (b) Doubleday, C.; McIver, J. W., Jr.; Page, M. *J. Phys. Chem.* **1988**, *92*, 4367−4371.

(4) (a) Yamaguchi, Y.; Schaefer, H. F., III; Baldwin, J. E. *Chem. Phys. Lett.* **1991**, *185*, 143. (b) Baldwin, J. E.; Yamaguchi, Y.; Schaefer, H. F., III *J. Phys. Chem.* **1994**, *98*, 7513. (c) Baldwin, J. E.; Freedman, T. B.; Yamaguchi, Y.; Schaefer, H. F., III *J. Am. Chem. Soc.* **1996**, *118*, 10934.

(5) (a) Getty, S. J.; Davidson, E. R.; Borden, W. T. *J. Am. Chem. Soc.* **1992**, *114*, 2085. (b) Borden, W. T.; Davidson, E. R. *J. Am. Chem. Soc.* **1980**, *102*, 5409.

(6) (a) Doubleday, C. *J. Phys. Chem.* **1996**, *100*, 15083−15086. (b) Doubleday, C. *Chem. Phys. Lett.* **1995**, *233*, 509. (c) Doubleday, C. *J. Am. Chem. Soc.* **1993**, *115*, 11968−11983. (d) Doubleday, C.; Camp, R. N.; King, H.; McIver, J., Jr.; Mullally, D.; Page, M. *J. Am. Chem. Soc.* **1984**, *106*, 447. (e) Doubleday, C.; Page, M.; McIver, J. W., Jr. *J. Mol. Struct. THEOCHEM* **1988**, *163*, 331.

(7) (a) Bernardi, F.; Bottoni, A.; Celani, P.; Olivucci, M.; Robb, M.; Venturini, A. *Chem. Phys. Lett.* **1992**, *192*, 229. (b) Bernardi, F.; Bottoni, A.; Robb, M.; Schlegel, H. B.; Tonachini, G. *J. Am. Chem. Soc.* **1985**, *107*, 2260. (c) Bernardi, F.; Bottoni, A.; Tonachini, G.; Robb, M.; Schlegel, H. B. *Chem. Phys. Lett.* **1984**, *108*, 599.

(8) Pedersen, S.; Herek, J. L.; Zewail, A. H. *Science* **1994**, *266*, 1359.

(9) (a) Carpenter, B. K. *J. Am. Chem. Soc.* **1996**, *118*, 10329. (b) Carpenter, B. K. *J. Am. Chem. Soc.* **1995**, *117*, 6336. (c) Carpenter, B. K. *Acc. Chem. Res.* **1992**, *25*, 520.

(10) Goldstein, M.; Cannarsa, M.; Kinoshita, T. Konitz, R. *Stud. Org. Chem. (Amsterdam)* **1987**, *31*, 121.

(11) Dervan, P.; Santilli, D. *J. Am. Chem. Soc.* **1980**, *102*, 3863.

(12) Hoffmann, R. *J. Am. Chem. Soc.* **1968**, *90*, 1475.

(13) Benson, S. W.; O'Neal, H. *J. Chem. Phys.* **1968**, *72*, 1866.

(14) (a) Horsley, J. A.; Jean, Y.; Moser, C.; Salem, L.; Stevens, R. M.; Wright, J. S. *J. Am. Chem. Soc.* **1972**, *94*, 279. (b) Salem, L. In *The New World of Quantum Chemistry*; Pullman, B., Parr, R. G., Eds.; Reidel: Dordrecht, 1976; p 241.

(15) Hay, P. J.; Hunt, W. J.; Goddard, W. A. *J. Am. Chem. Soc.* **1972**, *94*, 638.

(16) (a) Berson, J. A.; Pedersen, L. D. *J. Am. Chem. Soc.* **1975**, *97*, 238. (b) Berson, J. A.; Pedersen, L. D.; Carpenter, B. K. *J. Am. Chem. Soc.* **1976**, *98*, 122. (c) The authors thank Professor Berson for a helpful discussion of the dependence of k_{12}/k_1 on the isotope effect.

(17) (a) Cianciosi, S. J.; Ragunathan, N.; Freedman, T. B.; Nafie, L. A.; Lewis, D. K.; Glenar, D. A.; Baldwin, J. E. *J. Am. Chem. Soc.* **1991**, *113*, 1864. (b) Baldwin, J. E.; Cianciosi, S. J.; Glenar, D. A.; Hoffman, G. J.; Wu, I.; Lewis, D. K. *J. Am. Chem. Soc.* **1992**, *114*, 9408. (c) Freedman, T. B.; Cianciosi, S. J.; Ragunathan, N.; Baldwin, J. E.; Nafie, L. A. *J. Am. Chem. Soc.* **1991**, *113*, 8298. (d) Baldwin, J. E.; Cianciosi, S. J. *J. Am. Chem. Soc.* **1992**, *114*, 9401.

(18) An earlier experiment on (*S*,*S*)-**1** was reported by Baldwin and coworkers (Cianciosi, S. J.; Ragunathan, N.; Freedman, T. B.; Nafie, L. A.; Baldwin, J. E. *J. Am. Chem. Soc.* **1990**, *112*, 8204) that gave $k_i/k_\alpha = 1.09$. However, Baldwin later concluded (ref 2a) that the uncertainty in the data was too large to permit any mechanistically significant conclusions to be drawn from the double/single rate constant ratios.

(19) Our definition of single rotation is that of Baldwin (refs 2a and 17). Berson's definition of the single rotation rate constant in ref 16 included contributions from both C_1-C_2 and C_1-C_3 cleavage. In our notation, his single rotation rate constant would be equal to $k_1 + k_1'$.

(20) Baer, T.; Hase, W. L. *Unimolecular Reaction Dynamics: Theory and Experiments*; Oxford University Press: New York, 1996.

(21) (a) Truhlar, D.; Isaacson, A.; Garrett, B. In *Theory of Chemical Reaction Dynamics*; Baer, M., Ed.; CRC Press: Boca Raton, FL, 1985; Vol. IV, p 65. (b) Truhlar, D.; Garrett, B. *Acc. Chem. Res.* **1980**, *13*, 440. (c) Hase, W. L. *Acc. Chem. Res.* **1983**, *16*, 258.

(22) Chapuisat, X.; Jean, Y. *J. Am. Chem. Soc.* **1975**, *97*, 6325.

(23) Bolton, K.; Hase, W. L.; Peslherbe, G. H. In *Multidimensional Molecular Dynamics Methods*; Thompson, D. L., Ed; World Scientific: NJ, in press.

(24) (a) Doubleday, C.; Bolton, K.; Peslherbe, G. H.; Hase, W. L. *J. Am. Chem. Soc.* **1996**, *118*, 9922. (b) Bolton, K.; Hase, W. L.; Doubleday, C. *Ber. Bunsen-Ges. Phys. Chem.* **1997**, *101*, 414.

(25) (a) Helgaker, T.; Uggerud, E.; Jensen, H. *Chem. Phys. Lett.* **1990**, *173*, 145. (b) Uggerud, E.; Helgaker, T. *J. Am. Chem. Soc.* **1992**, *114*, 4265.

(26) Chen, W.; Hase, W. L.; Schlegel, H. B. *Chem. Phys. Lett.* **1994**, *228*, 436.

(27) Gordon, M. S.; Chaban, G.; Taketsugu, T. *J. Phys. Chem.* **1996**, *100*, 11512.

(28) Hase, W. L.; Duchovic, R. J.; Hu, X.; Komornicki, A.; Lim, K.; Lu, D.-h.; Peslherbe, G. H.; Swamy, K. N.; Vande Linde, S. R.; Wang, H.; Wolfe, R. J. VENUS 96, a General Chemical Dynamics Computer Program. *QCPE* **1996**, *16*, 671. VENUS 96 is an enhanced version of MERCURY: Hase, W. L. *QCPE* **1983**, *3*, 453.

(29) (a) Stewart, J. J. P. MOPAC 7.0, a General Molecular Orbital Package. *QCPE* **1993**, 455. (b) Stewart, J. J. P. *J. Comput. Chem.* **1989**, *10*, 209.

(30) Peslherbe, G. H.; Bolton, K.; Doubleday, C.; Hase, W. L. VENUS-MOPAC, a General Chemical Dynamics and Semiempirical Direct Dynamics Computer Program, to be released.

(31) Dewar, M. J. S.; Zoebisch, E. G.; Healy, E. F.; Stewart, J. J. P. *J. Am. Chem. Soc.* **1985**, *107*, 3902.

(32) Variational TST calculations using MOPAC with specific reaction path parameters have been reported in the following. (a) Gonzalez-Lafont, A.; Truong, T. N.; Truhlar, D. G. *J. Phys. Chem.* **1991**, *95*, 4618. (b) Liu, Y.-P.; Lu, D.-H.; Gonzalez-Lafont, A.; Truhlar, D. G.; Garrett, B. C. *J. Am. Chem. Soc.* **1993**, *115*, 7806.

(33) Doubleday, C.; Bolton, K.; Hase, W. L. *J. Am. Chem. Soc.* **1997**, *119*, 5251.

(34) Hrovat, D. A.; Fang, S.; Borden, W. T.; Carpenter, B. K. *J. Am. Chem. Soc.* **1997**, *119*, 5253.

(35) Dewar, M. J. S.; Hashmall, J. A.; Venier, C. G. *J. Am. Chem. Soc.* **1968**, *90*, 1953.

(36) Fukui, K. *J. Chem. Phys.* **1970**, *74*, 4161.

(37) Herek, J. L.; Zewail, A. H. To be published, quoted in ref 4c. The preliminary value in ref 8 was 120 ± 20 fs.

(38) Hase, W. L.; Buckowski, D. G. *J. Comput Chem.* **1982**, *3*, 335.

(39) Bunker, D. L.; Hase, W. L. *J. Chem. Phys.* **1973**, *59*, 4621.

(40) Pechukas, P. In *Dynamics of Molecular Collisions, Part B*; Miller, W. H., Ed.; Plenum Press: New York, 1976; p 269.

(41) Miller, W. H. *Acc. Chem. Res.* **1976**, *9*, 306.

(42) Truhlar, D. G.; Muckerman, J. T. In *Atom-Molecule Collision Theory*; Berstein, R. B., Ed.; Plenum: New York, 1979; Chapter 16.

(43) Porter, R. M.; Raff, L. M. In *Dynamics of Molecular Collisions, Part B*; Miller, W. H., Ed.; Plenum Press: New York, 1976; p 1.

(44) (a) Topaler, M.; Makri, N. *J. Chem. Phys.* **1992**, *97*, 9001. (b) Wyatt, R. E.; Iung, C.; LeForestier, C. *J. Chem. Phys.* **1992**, *97*, 3458, 3477. (c) Wyatt, R. E.; Iung, C. *J. Chem. Phys.* **1993**, *98*, 5191.

(45) Untch, A.; Schinke, R.; Cotting, R.; Huber, J. R. *J. Chem. Phys.* **1993**, *99*, 9553.

(46) Chen, W.; Hase, W. L.; Schlegel, H. B. *Chem. Phys. Lett.* **1994**, *228*, 436.

(47) Pollak, E.; Pechukas, P. *J. Am. Chem. Soc.* **1978**, *100*, 2984.

(48) The harmonic vibrational partition function for the nontorsional modes of Con‡, Dis‡, and CT‡ are negligibly different. The uniformly low torsional barriers at Con‡, Dis‡, and CT‡ imply nearly identical torsional partition functions for a given deuteration pattern. Conventional rather than variational TST is assumed.

(49) Page, M.; McIver, J. W., Jr. *J. Chem. Phys.* **1988**, *88*, 922.

(50) McQuarrie, D. A. *Statistical Thermodynamics*; University Science Books: CA, 1973.

(51) (a) Chapman, S.; Bunker, D. L. *J. Chem. Phys.* **1975**, *62*, 2890. (b) Sloane, C. S.; Hase, W. L. *J. Chem. Phys.* **1977**, *66*, 1523.

(52) Cho, Y. J.; Vande Linde, S. R.; Zhu, L.; Hase, W. L. *J. Chem. Phys.* **1992**, *96*, 8275.

(53) Bunker, D. L. *Methods Comput. Phys.* **1971**, *10*, 287.

(54) Bunker, D. L.; Goring-Simpson, E. A. *Faraday Discuss. Chem. Soc.* **1973**, *55*, 93.

(55) (a) Pulay, P. *Mol. Phys.* **1969**, *17*, 197. (b) Fogarasi, G.; Pulay, P. In *Vibrational Spectra and Structure*, 14th ed.; Durig, J. R., Ed.; Elsevier: Amsterdam, 1985; p 125. (c) Nguyen, K. A.; Jackels, C. F.; Truhlar, D. G. *J. Chem. Phys.* **1996**, *104*, 6491.

(56) Allen, M.; Tildesley, D. *Computer Simulation of Liquids*; Clarendon: Oxford, 1990.

(57) The ordering and assignments of the nontorsional modes are identical in CT‡, Con‡, and Dis‡. For a given mode below 1200 cm^{-1}, the largest variation in frequency is 40 cm^{-1}; above 1200 the variation rapidly decreases.

(58) Robinson, P. J.; Holbrook, K. A. *Unimolecular Reactions*; Wiley: London, 1972; p 152.

(59) Each methylene was rotated rigidly as a unit about the C−C bond during the sampling. Only the hydrogens were rotated, and all other internal coordinates were held fixed.

(60) Press, W. H.; Teukolsky, S. A.; Vetterling, W. T.; Flannery, B. P. *Numerical Recipes in Fortran; The Art of Scientific Computing*; University Press: Cambridge, 1992.

(61) Dewar, M. J. S.; Liotard, D. A. *J. Mol. Struct. THEOCHEM* **1990**, *206*, 123.

(62) C.D. is grateful to the Cornell Theory Center for a grant of computer time.

(63) The important qualitative differences are the following. (1) AM1-SRP incorrectly puts Dis‡ higher than CT‡; ref 34 has the correct ordering. (2) Reference 34 does not allow propene formation; AM1-SRP includes it. (3) In AM1−SRP, Dis‡ is a second-order saddle point; in ref 34 CT‡ is a second-order saddle point. On the ab initio PES both are first-order saddle points.

(64) (a) Schranz, H. W.; Raff, L. M.; Thompson, D. L. *J. Chem. Phys.* **1991**, *94*, 4219−4229. (b) Sewell, T. D.; Schranz, H. W.; Raff, L. M.; Thompson, D. L. *J. Chem. Phys.* **1991**, *95*, 8089.

(65) The TS criterion CCC = 94° was determined in ref 24a by Monte Carlo calculation of the relative sum of states as a function of geometry projected onto the CCC angle. However, this TS criterion was not used in the present calculations because nearly all trajectories initiated at CCC = 94° cyclize immediately without isomerization. This shows that the use of CCC = 94° as the sole TS criterion is not adequate at 695 K and suggests that the TS definition should include a larger number of coordinates and perhaps momenta as well.